




# Tracklet-to-object Matching for Climbing Starlink Satellites through Recursive Orbit Determination and Prediction

Bin Li<sup>1</sup> , Lei Liu<sup>1</sup>, and Ji-Zhang Sang<sup>1,2</sup>

<sup>1</sup> School of Geodesy and Geomatics, Wuhan University, Wuhan 430079, China; [lliu@sgg.whu.edu.cn](mailto:lliu@sgg.whu.edu.cn)

<sup>2</sup> Collaborative Innovation Center for Geospatial Technology, Wuhan 430079, China

Received 2022 May 24; revised 2022 September 6; accepted 2022 September 7; published 2022 October 19

## Abstract

Concerns for the collision risk involving Starlink satellites have motivated the interest in obtaining their accurate orbit knowledge. However, accurate orbit determination (OD) and prediction (OP) of Starlink satellites confront two main challenges: mismatching or missed matching of sparse tracklets to maneuvering satellites, and unknown or unmodeled orbit maneuvers. How to exactly associate a tracklet to the right satellite is the primary issue, since a maneuvering satellite does not follow the naturally evolving orbit during the maneuvering, while more tracklets are needed for developing an accurate orbit maneuver model. If these two challenges are not well addressed, it may lead to catalog maintenance failure or even loss of objects. This paper proposes a method to correctly match tracklets to the climbing Starlink satellites. It is based on the recursive OD and OP, in which the orbit maneuver is modeled and the thrust is estimated, such that the subsequent OP accuracy guarantees the correct match of tracklets shortly after the OD time. Experiments with climbing Starlink satellites demonstrate that the tracklets within three days of the last TLE (two-line element) are all correctly matched to the right satellites. With the matched tracklets, the thrust accelerations of climbing Starlink satellites can be precisely estimated through an orbit control approach, and the position prediction accuracy over 48 hours is at the level of a few kilometers, providing accurate orbit knowledge for reliable collision warning involving Starlink satellites.

*Key words:* celestial mechanics – methods: analytical – miscellaneous

## 1. Introduction

On 2022 July 24, SpaceX sent 53 Starlink satellites to the low-Earth-orbit (LEO) region, and the total number of Starlink satellites in orbit was 2923 then, according to the latest statistics in SATELLITE CATALOG at <https://www.space-track.org>. By 2022 July 30, the number of space objects tracked by the US Space Surveillance Network (SSN) was approximately 46,900, of which the population of the active payloads was 6300, referring to the SPACE SCOREBOARD at <https://www.space-track.org>. With the growing object population in near-Earth space, tracking, identifying, and cataloging space objects tend to be increasingly challenging, especially for the Starlink satellites because of their varying ballistic trajectories and fast-growing population. While space debris and active satellites, without propulsion abilities, are moving in their natural orbits, the Starlink satellites maneuver or climb continuously after launching. Even the deployed Starlink satellites, they maneuver frequently to maintain their working orbits. Such a large population of maneuvering Starlink satellites is inevitably involved in space safety events, such as the close approach between Starlink-1546 and OneWeb-017B on 2020 April 3 (<https://spacenews.com/spacex-and-oneweb-spar-over-satellite-close-approach>), and two close approaches between Starlink-1095/Starlink-2305 and China Space Station

on 2021 July 1/October 21 (<https://spacenews.com/chinas-space-station-maneuvered-to-avoid-starlink-satellites>), respectively.

Potential threats from the Starlink satellites demand the space situational awareness (SSA) community have an accurate and timely knowledge of their orbit information. In the orbit dynamics field, a space object is solely characterized by a six-dimensional orbital state vector (position and velocity, or Keplerian orbital elements). Its accuracy is closely related to the availability of tracking data, orbit propagation method, and perturbation force models (Montenbruck & Gill 2000). To be specific, an accurate orbit state can be obtained through orbit determination (OD), in which the initial orbit state and some of the force model parameters are adjusted to best fit the available observations. Then, the orbit prediction (OP) starts by propagating the orbit solutions to the future time using analytical or numerical methods. Such an OD/OP process is usually applicable to a space object of ballistic or natural trajectory, as its orbit dynamics characteristics can be precisely modeled. More importantly, its tracklets, short orbit arcs observed by ground-based or space-based sensors, can be easily associated (Cai et al. 2018; Lei et al. 2018; Liu et al. 2021). However, for the maneuvering Starlink satellites, identifying the object attribution of the tracklets is more difficult, since their exact orbit maneuvering operations are unknown to the public. Even though the tracklets are

successfully identified, the lack of an accurate thrust model could lead to OD failure.

In the LEO region, the classical orbit maneuver technique of the active satellites refers to the thrust to overcome the degradation effect of the atmospheric drag. While in all orbit regions, orbit maneuver occurs mainly for collision avoidance, orbit altitude/attitude control, orbit transfer, and so on. These maneuvers are generally categorized as impulsive maneuvers and continuous low-thrust maneuvers (Vallado 2007). In the case of an impulsive maneuver occurs, the position of the spacecraft is considered to be fixed and the velocity is changed instantaneously. While the continuous low-thrust maneuver changes the momentum of the spacecraft slowly over a long time by electrically-powered propulsion rather than by a short impulse. Generally, the effect of low thrust can be well absorbed by some parameters in the OD, when the tracking data is sufficient and well-distributed both temporally and spatially.

However, in the routine ground-based radar or optical tracking scenarios, usually only short or even very short tracklets of the Starlink satellites are observed, with their durations from a few seconds to several minutes, which are very short relative to their orbital periods (Jiang et al. 2017). More commonly, these tracklets are mainly from a single station, very sparse in the temporal and spatial distribution. These tracklets are mixed with the ones of other objects (space debris and satellites). As a result, accurate OD and OP of a maneuvering Starlink satellite is a very real challenging problem. The primary difficulty comes from the tracklet-to-object correlation since a maneuvering satellite does not follow the natural orbit while the tracklet covers only a very small portion of the whole orbit. For example, if the last two-line element (TLE) of the observed Starlink satellite is not of good quality or released a few days earlier, the tracklet-to-object correlation method based on the  $O-C$  test, discussed in Section 2.1, would be incapable of pairing the tracklet to the right satellite, as the accuracy of TLE-predicted position with the Simplified General Perturbation 4 (SGP4) model drops very quickly, with the 1-day position prediction error at an order of kilometers to dozens of kilometers. Alternatively, the satellite operator delivers the precise orbit ephemerides of Starlink satellites via the Internet at <https://www.space-track.org/#publicFiles>. But, without any knowledge of the maneuver force model, the OP based on precise ephemeris with the conventional orbit propagation method would still result in large errors in the predicted positions. More seriously, the cataloged orbits of the Starlink satellites maybe not timely accessible due to delivery delay, network breakdown, or object loss. Additionally, measurement errors will cause the difficulty of tracklet-to-object correlation for the maneuvering Starlink satellites. Radar tracking is the most popular space surveillance technique for the cataloging of LEO objects, while the cataloging of GEO objects is mainly based on optical observation. The measurement error is in the order of tens of meters/arcseconds for the radar range/angle observations, according to the performance of

ground-based radar in Table 4-4 in Vallado (2007). Especially, a batch of Starlink satellites are closely spaced for a short time after launching, called the group target. This could very likely lead to the problem that a tracklet is matched to multiple Starlink satellites, because of the low accuracy in both the radar angles and TLE predictions.

Focusing on the problem of tracklet-to-object matching for maneuvering satellites, various methods have been explored. Huang et al. (2012) mathematically formulated the object correlation and maneuver detection problem as a maximum a posterior (MAP) estimation and proposed an approach to solving the MAP estimation. Holzinger et al. (2012) demonstrated the utility of control metrics to correlate object observations, and detect and correlate tracklets for unknown objects via hypothesis testing and non-Gaussian boundary condition. Siminski et al. (2017) proposed two methods for the correlation and orbit recovery for unknown maneuver strategies, including using an admissible region, a predetermined region that the orbit is likely located in, and characterizing the historic maneuver data to compute the association likelihood and predict the most likely state after a maneuver. Serra et al. (2021) applied the optimal control theory to tackle the tracklet-to-orbit association in the presence of an unknown maneuver, in which the admissible region is combined with the control theory to determine the tracklet-to-orbit association.

The problem of detecting and estimating an unknown maneuver has attracted wide attention over the decades. Kelecý & Jah (2010) studied the performance of the batch least-squares (BLS) and extended Kalman filter (EKF) in detecting and assessing low thrust satellite maneuvers. Zhai et al. (2018) developed a variable structure estimator to deal with the orbit determination and propagation of maneuvering satellites. Once a maneuver is observed or detected, the EKF is expanded to include variables to account for the effect of the maneuver on the satellite state. Also, a variable state dimension (VSD) estimator was developed to address the relative position determination problem of the non-cooperative target subjected to constant unknown maneuvers (Zhai et al. (2019)). For real-time tracking of a non-cooperative and maneuvering spacecraft, an Interacting Multiple Model (IMM) OD filter was proposed by Goff et al. (2015). Essentially, the filter is adaptive to observations through the inflation of state covariance such that the state estimates are converged to the real-time tracking observations. An adaptive state estimation algorithm based on multiple EKF filters along with the IMM was developed to perform the orbit determination and prediction of spacecraft with and without impulsive maneuvers (Lee et al. 2016). The ability to predict impulsive maneuvers more accurately was shown such that more accurate state estimations were achieved. In addition, great efforts have been made in detecting and estimating the maneuvers and orbital anomalies for GNSS satellites, by using the GNSS data (Qiao & Chen 2018), the ephemeris data (Tu et al. 2021), and predicted clock

information (Dai et al. 2019). These studies are just examples of how to deal with the problems of maneuver detection and estimation, and there could be other options, too, for example using a UKF (Unscented Kalman Filter) instead of an EKF. However, different from the above, the tracklet-to-object association problem of Starlink satellites is much more challenging, in terms of the number of satellites, maneuvering duration and frequency, maneuvering mode, tracking data accuracy and availability, and the TLE update rate.

In this paper, an effective and practical tracklet-to-object matching method is developed for the climbing Starlink satellites. It is based on the  $O-C$  test, but the application of the recursive OD strategy, in which newly matched tracklets are used, makes sure the OP accuracy is sufficient for the tracklet-to-object association within a day or two days after the OD time. In the implementation of this strategy, the tracklet-to-object association is performed only for the tracklets within one day of the last correctly matched tracklet, in which the recursive OD/OP result using the last matched tracklet is used to compute the theoretical observations. This process continues until the tracklets of a maneuvering Starlink satellite are all correctly correlated. In each tracklet-to-object matching process, the previous reference orbit is modified by the use of the matched tracklets through orbit estimation, which in turn contributes to more reliable tracklet-to-object matching.

The rest of this article starts with the description of object matching based on the  $O-C$  test in Section 2. In Section 3, the framework of the accurate OD using sparse tracklets is developed, in which the estimation of thrust model parameters is considered. In Section 4, the data processing results of Starlink satellites are presented and analyzed. Finally, Section 5 concludes this article.

## 2. Object Matching

The purpose of object matching is to determine which space object a tracklet belongs to. Thus, if the tracklets identification is known, it can be used to update the orbit. Considering the maneuvering features of Starlink satellites, purely comparing the orbit elements derived by the tracklet to the cataloged orbit elements would result in false matching or missed matching (Wang et al. 2016). In this section, a high-accuracy object matching method based on the  $O-C$  test is proposed for the maneuvering Starlink satellites, including two main steps: rough matching with cataloged TLE orbit and precise matching with autonomous orbit.

### 2.1. $O-C$ Test

A radar tracklet consists of a series of observations  $O$  containing the azimuth angle  $Az$ , elevation angle  $El$ , and range  $\rho$ . According to the radar angle and range observational model, the theoretical observations  $C$  at the observing time epoch can be computed, given the radar station location and the space

objects orbital state. The main idea of object matching based on the  $O-C$  test is to compare  $O$  with  $C$ . If  $|O - C|$  is less than a pre-set matching threshold, the tracklet is regarded as belonging to the space object whose orbit has been used to compute  $C$ ; otherwise, the tracklet comes from another object. If the tracklet fails to match a cataloged space object, it belongs to an unknown object or an uncatalogued object.

Given the initial orbit state of a space object before the radar tracking time, the theoretical observation  $C$  at the observing epoch is computed as

$$C_{Az} = \tan^{-1} \frac{(\mathbf{r}_{t_s} - \mathbf{r}_{t_r}) \cdot \mathbf{E}}{(\mathbf{r}_{t_s} - \mathbf{r}_{t_r}) \cdot \mathbf{N}} \quad (1)$$

$$C_{El} = \sin^{-1} \frac{(\mathbf{r}_{t_s} - \mathbf{r}_{t_r}) \cdot \mathbf{U}}{|\mathbf{r}_{t_s} - \mathbf{r}_{t_r}|} \quad (2)$$

$$C_{\rho} = |\mathbf{r}_{t_s} - \mathbf{r}_{t_r}| + |\mathbf{r}_{t_s} - \mathbf{r}_{t_r}| \quad (3)$$

where  $t_f$ ,  $t_s$ , and  $t_r$  are the times of radar signal transmitted from the station, arrived at the object, and returned to the station, respectively;  $\mathbf{r}_{t_f}$  and  $\mathbf{r}_{t_r}$  are the station position vectors at  $t_f$ ,  $t_r$ , respectively;  $\mathbf{r}_{t_s}$  is the object position vector at  $t_s$ ;  $(\mathbf{N}, \mathbf{E}, \mathbf{U})$  denotes the unit vectors in the horizontal north direction, horizontal east direction, and zenith direction at the station.

In Equations (1)–(3),  $\mathbf{r}_{t_f}$  and  $\mathbf{r}_{t_r}$  can be easily computed through the station coordinate transformation. While  $\mathbf{r}_{t_s}$  is obtained by integrating the equations of motion of the object forward with the initial orbit state vector of the object and assumed force model parameters. The integration is either numerical or analytical, depending on the type of the given initial orbit state. Its accuracy heavily relies on the accuracy of the initial orbit state, orbit propagation method, the dynamic models, and the OP time length (Montenbruck & Gill 2000).

For the radar observation at the  $i$ th epoch, the deviation  $v$  between  $O$  and  $C$  is computed as

$$\Delta_{Az,i} = O_{Az,i} - C_{Az,i} \quad (4)$$

$$\Delta_{El,i} = O_{El,i} - C_{El,i} \quad (5)$$

$$\Delta_{\rho,i} = O_{\rho,i} - C_{\rho,i} \quad (6)$$

where  $\Delta_{Az,i}$ ,  $\Delta_{El,i}$ , and  $\Delta_{\rho,i}$  denote the difference of azimuth angle, elevation angle, and range between the real radar observations and its theoretical values, respectively.

In the radar tracking scenario, hundreds of thousands of tracklets can be collected once the space objects go through the field of view of the radar sensor. It is extremely time-consuming to compute  $\Delta$  for each observation of all tracklets, since the computation of space object position  $\mathbf{r}_{t_s}$  at the observing time epoch needs extensive orbit integration and numerical interpolation. To improve the computation efficiency of object matching, the object visibility with respect to the station during the radar tracking period is analyzed first. For a given tracklet of  $N$  observation epochs, five epochs at or near  $t_1$ ,  $t_{N/4}$ ,  $t_{N/2}$ ,  $t_{3N/4}$ , and  $t_N$ , are chosen to compute  $\Delta$ , which results in the time series

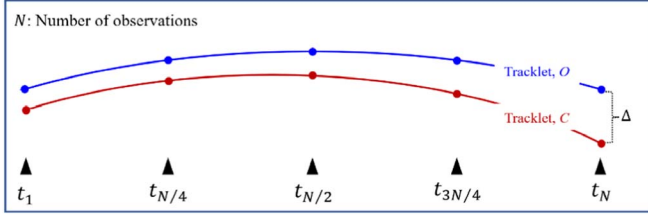


**Figure 1.** Observation point-selection in the computation of  $\Delta$  for a tracklet with  $N$  observations.

of observation deviation, as illustrated in Figure 1. If the absolute  $\Delta$  values at these epochs are all less than preset thresholds, then  $\Delta$  values at all epochs are computed. It is noted that a data cleaning should be done beforehand to avoid the pollution of observation outliers on the accuracy of  $\Delta$ . The data cleaning is mainly to detect and remove outliers in the observations, in which the usual 3-sigma threshold is applied.

After getting the  $\Delta$  time series for a single tracklet, the root mean square (rms) values of the angle and range deviations are computed as

$$\text{RMS}_{A_z} = \sqrt{\frac{1}{N} \sum_{i=1}^N (\Delta_{A_z,i} \times \cos El_i)^2} \quad (7)$$

$$\text{RMS}_{El} = \sqrt{\frac{1}{N} \sum_{i=1}^N \Delta_{El,i}^2} \quad (8)$$

$$\text{RMS}_\rho = \sqrt{\frac{1}{N} \sum_{i=1}^N \Delta_{\rho,i}^2} \quad (9)$$

where  $El_i$  is the elevation angle of the object at the  $i$ th epoch.

Conditions that a tracklet belongs to a cataloged object are

$$\text{RMS}_{A_z/El} < \Theta_{A_z/El} \quad (10)$$

$$\text{RMS}_\rho < \Theta_\rho \quad (11)$$

where  $\Theta_{A_z/El}$  and  $\Theta_\rho$  are the matching thresholds for the radar angle and range, respectively. If Equations (10) and (11) are satisfied, the tracklet is regarded as belonging to the object, and the tracklet can be used to update the orbit of the matched object through OD. However, there may exist multiple satellites matched to a single tracklet. In this case, the object with the minimum  $\text{RMS}_\rho$  is selected as the final matched satellite, since the radar ranging observations are more accurate, compared with the angular observations.

## 2.2. Tracklet-to-object Matching

The orbit maneuvering characterization of Starlink satellites makes its TLE have a short validity time for the OP, usually less than one day. This causes difficulty when matching tracklets to objects over several days after the TLE reference time. Meanwhile, the low accuracy of TLE predictions may lead to many mismatching tracklets or missed matches. In this sense, a reliable tracklet-to-object matching should be performed with a more accurate reference orbit. In this study,

the accurate reference orbit is produced from the OD/OP with the matched tracklets, defined as the autonomous orbit.

Currently, the North American Aerospace Defense Command (NORAD) TLE catalog is the sole public source of cataloged objects. To preliminarily judge the tracklets object attribution, the rough matching based on the  $O-C$  test is conducted first, in which the TLE orbit is used as the reference orbit. To have high reliability of the rough matching, only the position predictions within the first day of the TLE reference time are used.

After the rough match, the number of tracklets possibly belonging to the object is significantly reduced, and the precise matching can proceed. Assuming there are  $k$  ( $k \geq 1$ ) tracklets roughly matched to a Starlink satellite,  $k$  OD runs, each using a rough-matched tracklet, are performed to extend the time of validity of the TLE orbit. In this OD operation, the first initial orbit state is computed by the TLE, and the orbit propagation method is the analytic SGP4. More details about the TLE/SGP4-based OD, named the TLE-OD, can be referred to our previous studies (Li et al. 2016; Sang et al. 2017). The superiority of TLE-OD is that it can converge easily and quickly, compared to the BLS OD. Although there are  $k$  roughly matched tracklets, only the OD with the smallest residual rms is accepted as the improved TLE, because the use of wrongly matched tracklets will cause TLE-OD to fail or to converge with very large residual rms.

In fact, the improved TLE still has limited validity time. Also, the SGP4 model is not able to accurately account for the continuous low thrust effect on the Starlink satellite during the maneuvering period. There may be still some tracklets not matched after the above process. To find the missed tracklets, an OD process is performed again. Different from the TLE-OD process, in this procedure, the BLS OD using the numerical orbit propagation method is performed, since some tracklets have already been correctly matched. The initial orbit state for the BLS OD is the improved TLE. To account for the atmospheric drag and thrust effect on the orbit, the drag coefficient and the thrust model parameters are also estimated in the BLS OD, which will be discussed in Section 3. In this case, with more accurate orbit information, the missed tracklets can be found, and they are used to further improve the OD accuracy which helps in the subsequent tracklet-to-object matching. This process ends until the number of matched tracklets of a Starlink satellite no longer increases. Figure 2 illustrates the implementation of the recursive tracklet-to-object matching method. It is noted that only TLEs of the Starlink satellites are used in the rough tracklet-to-object matching. It is also noted that there is a step of tracklet matching using the TLE-OD results in Figure 2, such that more tracklets can be matched to the right satellite, which is needed in the subsequent BLS OD.

## 3. BLS OD Considering Thrust Model Parameters

The object matching provides available tracklets for the OD and subsequent OP. For the Starlink satellites, the orbit



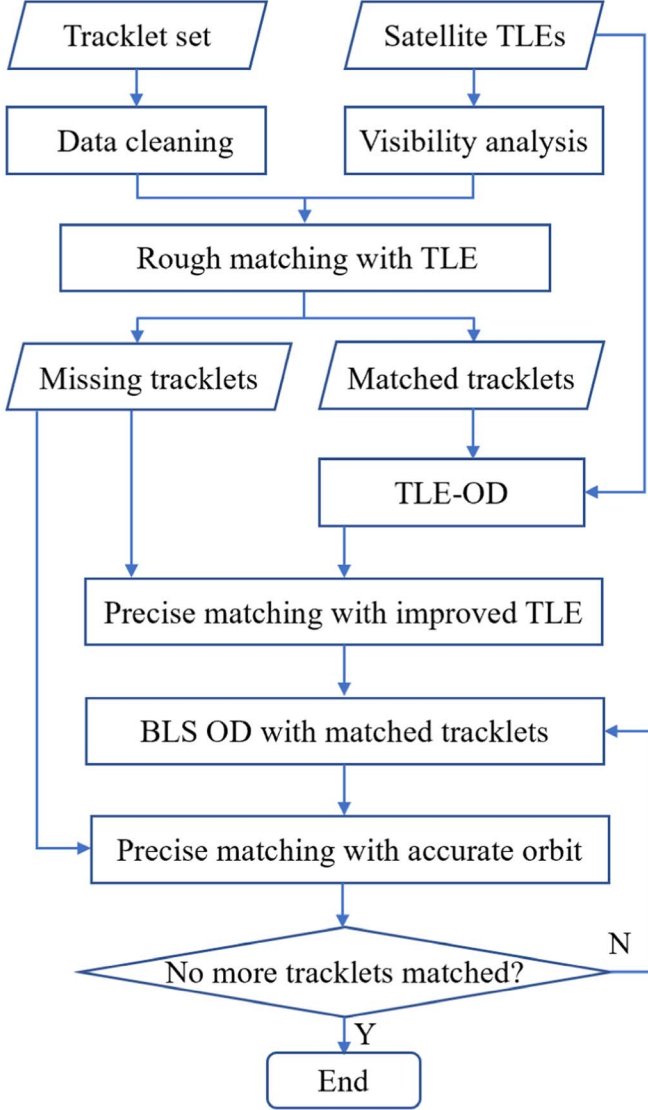


**Figure 2.** Implementation of the tracklet-to-object matching for maneuvering Starlink satellites.

maneuvering makes the traditional BLS OD method (Vallado 2007; Li et al. 2020) difficult to work. To achieve accurate OD results, the thrust force must be included in the orbit dynamics system when propagating the equations of motion. In this section, the BLS OD considering the thrust model for the maneuvering Starlink satellite is studied.

### 3.1. Orbit Dynamics

Considering the maneuver, the equations of motion of a satellite in the Earth-centered inertial (ECI) coordinate system can be expressed as

$$\ddot{\mathbf{r}} = -\mu \frac{\mathbf{r}}{r^3} + \mathbf{a}_{\text{per}} + \mathbf{\Gamma} \quad (12)$$

where  $\mathbf{r}$  and  $\ddot{\mathbf{r}}$  are the position and acceleration vectors of the satellite in the ECI coordinate system, respectively;  $r = \|\mathbf{r}\|$  with  $\|\cdot\|$  denoting the Euclidean norm of a vector;  $\mu$  is the Earth gravitational constant, and  $\mu = GM$ ;  $\mathbf{a}_{\text{per}}$  is the perturbation acceleration vector caused by the non-spherical gravity, third-body gravity attraction, atmospheric drag, and solar radiation pressure;  $\mathbf{\Gamma}$  is the thrust acceleration vector.

Examination of the orbit altitude variations during the climbing period reveals that a Starlink satellite would climb continuously from its parking orbit at the orbit altitude of about 350 km to the operational orbit at the altitude of 550 km, with its orbital altitude almost linearly increasing with time. This indicates that  $\mathbf{\Gamma}$  is generated by a continuous low-thrust. To fully account for the thrust effect on the satellite, a general acceleration model is assumed for the continuous low-thrust, expressed as

$$\mathbf{\Gamma} = \mathbf{M}_{\text{RSW} \rightarrow \text{ECI}} \cdot \begin{bmatrix} \Gamma_R \\ \Gamma_S \\ \Gamma_W \end{bmatrix} \quad (13)$$

where  $\Gamma_R$ ,  $\Gamma_S$ , and  $\Gamma_W$  denote the radial, along-track, and cross-track thrust accelerations in the RSW coordinate system, in which the  $R$  axis points from the Earth's center along the radius vector toward the space object, the  $S$  axis is normal to the position vector and positive in the direction of the velocity vector, and the  $W$  axis is normal to the orbital plane (Vallado 2007);  $\mathbf{M}_{\text{RSW} \rightarrow \text{ECI}}$  is the matrix which transforms the RSW coordinate system to the ECI coordinate system.

Analyzing the variation of TLE orbit elements of the maneuvering Starlink satellites shows that the orbital inclinations of Starlink satellites remain unchanged, indicating that the maneuver is only in the orbital plane, thus,  $\Gamma_W = 0.0 \text{ m s}^{-2}$ . This can be also seen in Table 1, in which the orbital inclination of the climbing Starlink satellite remains the same over three days.

To account for the almost constant altitude rising speed, both  $\Gamma_R$  and  $\Gamma_S$  are assumed constant over a few days, which can be estimated in the BLS OD. More importantly, this assumption is beneficial to OD convergence when only sparse tracklets are available.

### 3.2. Orbit Estimation Method

A weighted sum of squares of residuals (WSSR) is finally computed when all the matched tracklets are used in the orbit estimation.

$$\text{WSSR} = \sum_{i=1}^n (P_{Az,i} \Delta_{Az,i}^2 + P_{El,i} \Delta_{El,i}^2 + P_{\rho,i} \Delta_{\rho,i}^2) \quad (14)$$

where  $n$  is the number of available observations in the OD;  $P_{Az,i}$ ,  $P_{El,i}$  and  $P_{\rho,i}$  denote the weights of the radar azimuth, elevation, and range observations at the  $i$ th epoch, characterizing their relative accuracy;  $\Delta_{Az,i}$ ,  $\Delta_{El,i}$  and  $\Delta_{\rho,i}$  are the residuals of the radar azimuth, elevation, and range at the  $i$ th

**Table 1**  
Reference Orbit Parameters of the Climbing Starlink-48675 within the OD Fit Span

Epochs	Orbit Altitude(km)	Eccentricity	Inclination(deg)	RAAN(deg)
Day 1, 00:00:00	488.909	0.000 129	53.047	119.984
Day 2, 00:00:00	494.877	0.000 134	53.047	115.380
Day 3, 00:00:00	500.846	0.000 136	53.047	110.767
Day 3, 23:59:59	506.806	0.000 139	53.047	106.179

epoch, computed by Equations (4)–(6), given the initial orbit state  $\mathbf{x}_0$  and related dynamic models. The weight for the range is usually set to 1, and the weight for the angle is set as  $P_{Az,i} = P_{El,i} = \sigma_\rho^2 / (\sigma_{Az/El} \cdot \rho_i)^2$ , where  $\sigma_{Az/El}$  and  $\sigma_\rho$  are the standard deviations of the angle and range errors, respectively.

For a maneuvering Starlink satellite, the dynamic model parameters of the drag coefficient  $C_d$  and the thrust model parameters ( $\Gamma_R, \Gamma_S$ ) are estimated, in which  $C_d$  accounts for the drag effect, and ( $\Gamma_R, \Gamma_S$ ) for the thrust effect. Therefore, WSSR is a function of  $[\mathbf{x}_0, C_d, \Gamma_R, \Gamma_S]$ . In the sense of the BLS OD, the optimal estimations of  $[\mathbf{x}_0, \mathbf{p}]$ ,  $\mathbf{p} = (C_d, \Gamma_R, \Gamma_S)$ , are obtained by minimizing WSSR, expressed as

$$\hat{\mathbf{x}}_0 = \mathbf{x}_0 + \Delta\mathbf{x}_0, \hat{\mathbf{p}} = \mathbf{p} + \Delta\mathbf{p} \quad (15)$$

where

$$[\Delta\mathbf{x}_0, \Delta\mathbf{p}]^T = (\mathbf{B}^T \mathbf{P} \mathbf{B})^{-1} \mathbf{B}^T \mathbf{P} \mathbf{l} \quad (16)$$

$$\mathbf{B} = \frac{\partial \mathbf{H}}{\partial \mathbf{x}_t} \cdot \left[ \frac{\partial \mathbf{x}_t}{\partial \mathbf{x}_0} \quad \frac{\partial \mathbf{x}_t}{\partial \mathbf{p}} \right] = \mathbf{H}_{t,t} \cdot [\Phi_{t,t_0} \quad \mathbf{S}_t] \quad (17)$$

where  $\Delta\mathbf{x}_0, \Delta\mathbf{p}$  are the optimal corrections to  $[\mathbf{x}_0, \mathbf{p}]$ ;  $\mathbf{B}$  is the error equation matrix;  $\mathbf{P}$  is the weight matrix of the used observations, usually a diagonal matrix constructed by its observation variance;  $\mathbf{l}$  is the observation residual vector;  $\mathbf{H}_{t,t}$  is the observation matrix,  $\mathbf{H}_{t,t} = \frac{\partial \mathbf{H}}{\partial \mathbf{x}_t}$ ;  $\Phi_{t,t_0}$  is the state transition matrix,  $\Phi_{t,t_0} = \frac{\partial \mathbf{x}_t}{\partial \mathbf{x}_0}$ ;  $\mathbf{S}_t$  is the sensitivity matrix,  $\mathbf{S}_t = \frac{\partial \mathbf{x}_t}{\partial \mathbf{p}}$ .

The BLS OD is an iterative process, which ends when the change between the estimated  $\hat{\mathbf{x}}_0$  and its previous estimate is less than a pre-set converge threshold.

### 3.3. Initialization of Thrust Acceleration

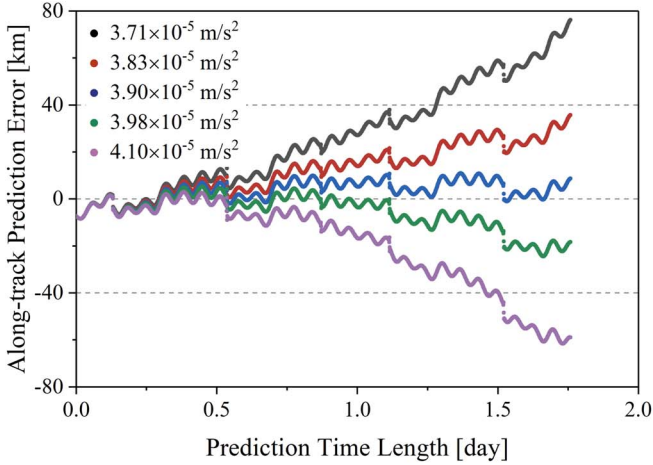
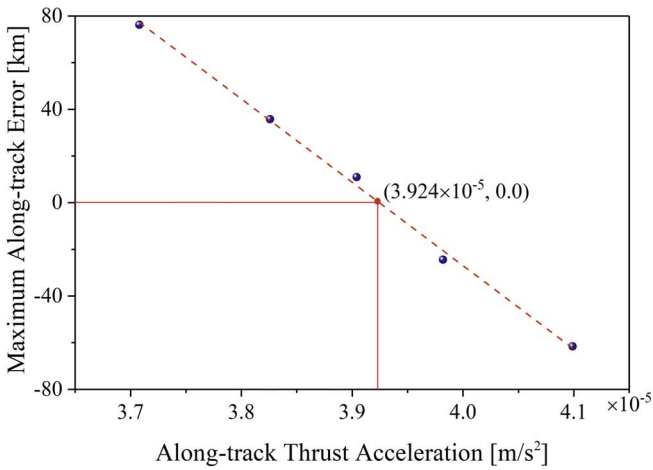
For a maneuvering satellite, the accuracy of orbit estimation is strongly dependent on the availability of tracklets and the appropriateness of the employed force models. To guarantee the convergence of the BLS orbit estimation,  $\mathbf{x}_0$  usually comes from the latest TLE or the previous OD result, and the initial value of  $C_d$  is set to 2.2 if there is no a priori information. By contrast, the initial values of  $\Gamma_R$  and  $\Gamma_S$  are not readily available. A small variation in the initial values of  $\Gamma_R$  and  $\Gamma_S$  could cause the propagated orbit to deviate significantly from its true orbit, due to the cumulative effect of thrust. Since the along-track thrust is the main driving force for raising the Starlink satellite orbit, the value of  $\Gamma_S$  should be well initialized, which is discussed below.

Figure 3 gives an example of how the error of  $\Gamma_S$  affects the along-track position prediction error  $e_S$  of the climbing Starlink satellite (NORAD ID: 48 661) between 2021 July 28, and 2021 July 30. In the orbit propagation computation, the Earths gravity, third-body gravities, atmospheric drag, solar radiation pressure, and thrust are all considered. The initial orbit state is the one at the first epoch of a precise ephemeris file. The Joint Gravity Model (JGM)-3 model (Tapley et al. 1996) with the full orders/degrees is used to compute the Earths gravitational force. The Jet Propulsion Laboratory (JPL) DE406 planetary ephemeris is used to compute the positions of the third bodies (Standish 1998). The NRLMSISE-00 atmospheric mass density model (Picone et al. 2002) is applied to compute the drag effect. The constant low-thrust model in Section 3.1 is used to compute the thrust effect. The SpaceX ephemeris is used to assess OP accuracy. Five values are assumed for  $\Gamma_S$  to demonstrate the relationship between  $\Gamma_S$  and  $e_S$ .

In Figure 3(a), the growth of  $e_S$  varies with different  $\Gamma_S$  values. For the case  $\Gamma_S = 3.90 \times 10^{-5} \text{ m s}^{-2}$ ,  $e_S$  has the lowest growth speed, with its maximum value, denoted as  $\max e_S$ , at 8.67 km within about 2 days, as shown in Figure 3(b). While for the other four cases,  $\max e_S$  exceeds 20 km. In particular, for the cases  $\Gamma_S = 3.71 \times 10^{-5} \text{ m s}^{-2}$  and  $\Gamma_S = 4.10 \times 10^{-5} \text{ m s}^{-2}$ ,  $\max e_S$  reaches 76.26 km and  $-58.92 \text{ km}$ , respectively, indicating that, when the value of  $\Gamma_S$  differs from its truth by a large margin, the predicted orbit will significantly deviate from the truth orbit. From the  $e_S$  growth trends of the five cases, it can be deduced that the true value of  $\Gamma_S$  is close to  $3.90 \times 10^{-5} \text{ m s}^{-2}$ , if the SpaceX ephemeris is accurate.

At the present, the models of the Earth gravity, third-body gravities, and solar radiation pressure are considered accurate in approximating the orbit dynamics of the SpaceX ephemeris, leaving the thrust and atmospheric drag as the main error sources for the OD and OP. In the climbing period of Starlink satellites, the thrust dominates the drag. By adjusting the value of  $\Gamma_S$  to reduce  $e_S$ , a reasonably accurate initial approximation of  $\Gamma_S$  can be obtained. This is shown in Figure 3(b) when the values of  $\Gamma_S$  and the corresponding  $\max e_S$  are plotted. An interesting finding is that there is a linear relationship between them. Through linearly fitting the  $(\Gamma_S, \max e_S)$  series, the value of  $\Gamma_S$  that leads to zero value of  $e_S$  can be estimated. In this case,  $\Gamma_S = 3.924 \times 10^{-5} \text{ m s}^{-2}$  is the appropriate initial value of  $\Gamma_S$ .

However, the BLS OD of a maneuvering Starlink satellite confronts two main problems: (1) how to accurately determine


 (a)  $e_S$  varies with  $\Gamma_S$ 

 (b)  $\max e_S$  with respect to different  $\Gamma_S$ .

**Figure 3.**  $e_S$  and  $\max e_S$  with respect to  $\Gamma_S$  for the climbing Starlink satellite (NORAD ID: 48 661) between 2021 July 28 and 2021 July 30.

a reasonably accurate range within which the true value of  $\Gamma_S$  should be located; (2) there may be no precise ephemeris available to compute  $e_S$ .

For the first problem, it can be tackled by using the TLE  $B^*$  parameter. In theory, it is a positive value when the satellite is in the LEO region where the drag is dominant. However, it is found that  $B^*$  is negative for the climbing Starlink satellites. It is understandable that the  $B^*$  parameter of the climbing satellite contains both the drag and the along-track thrust information. Extensive experiments with multiple climbing Starlink satellites show that initial  $\Gamma_S$  can be estimated as  $\Gamma_S^0 = -9.3 \times 10^{-4} \cdot B^* \text{ m s}^{-2}$ . The empirical equation is determined by using the precise ephemerides of the climbing Starlink satellites. As Figure 3(b) shows, the likely correct value of  $\Gamma_S$  can be estimated by letting  $e_S$  equal to zero. After the estimate of initial  $\Gamma_S$ , it is related to  $B^*$  with a simple equation of  $\Gamma_S = q \cdot B^*$ . With known  $B^*$  and estimated  $\Gamma_S$ ,  $q$  is determined

to be  $-9.3 \times 10^{-4}$ . The results show that Starlink satellites with different orbit raising speeds have very close  $q$  values. Thus, the constant value of  $q = -9.3 \times 10^{-4}$  is adopted to determine the initial value of  $\Gamma_S^0$ . Next, the accurate value of  $\Gamma_S$  is very likely within  $[0.95 \times \Gamma_S^0, 1.05 \times \Gamma_S^0]$ .

As for the second problem, assuming that the available tracklets cover  $m(m \geq 1)$  days, the tracklets in the first  $m - 0.5$  days are used in the BLS OD, while the remaining tracklets in the last 0.5 days are used as the reference to compute the prediction errors.

## 4. Experimental Results

The proposed tracklet-to-object matching algorithm for the climbing Starlink satellites is validated using ground-based radar observations. The radar observing accuracy is 50 m for the range and 100 arcseconds for the angles (Liu et al. 2021). The NORAD TLEs are used in the initial matching. The SpaceX ephemerides are used as the truth orbit to compute the OD and OP error. The SpaceX ephemeris file, containing three-day positions and velocities in the J2000 coordinate system, is updated three times daily. Only the orbit data from the first 8 hours in each ephemeris file is used since they are more accurate than those of later times. A precise orbit of a climbing Starlink satellite is produced by combining the positions and velocities of consecutive ephemeris files.

### 4.1. Starlink Orbit Characteristics

#### 4.1.1. Orbit Distribution

Analyzing the TLEs of current Starlink satellites reveals that, they are mainly in the orbit region of the altitude of 290 km–570 km (including the climbing satellites), and the orbit inclinations are about  $53^\circ 0$ ,  $70^\circ 0$ , and  $97^\circ 6$ , respectively. The distribution of the orbit semimajor axes and inclinations of all Starlink satellites on 2022 May 23 is presented in Figure 4.

It is found that the orbital planes are evenly distributed along the equator in terms of the right ascension of ascending node (RAAN), while in an orbital plane of the same RAAN, there are about 20 Starlink satellites evenly distributed. The position of a satellite in orbit can be measured by the phase angle  $\omega + f$  ( $\omega$ : argument of perigee;  $f$ : true anomaly), as shown in Figure 5.

#### 4.1.2. Orbit Variation

A typical feature of a batch of Starlink satellites in the same orbit plane is that they rise successively after launching. To describe the orbit-raising process, 20 Starlink satellites from the same launch in the same orbital plane are chosen from the TLE catalog. Their raising process is illustrated by the variations of orbit altitudes and phase angles with time, as shown in Figure 6.

In Figure 6(a), the satellites climb from an initial orbit altitude of about 350 km to the destined orbit altitude of

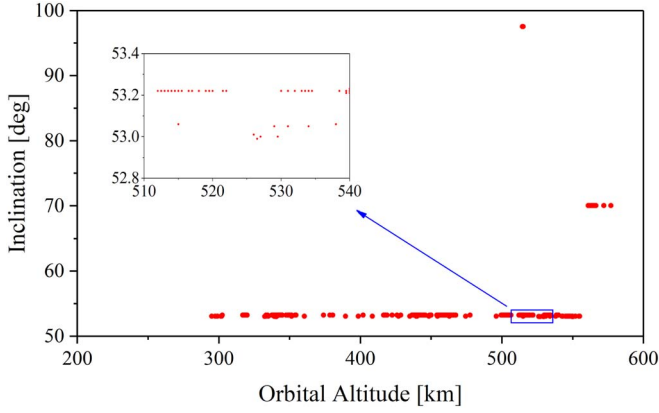


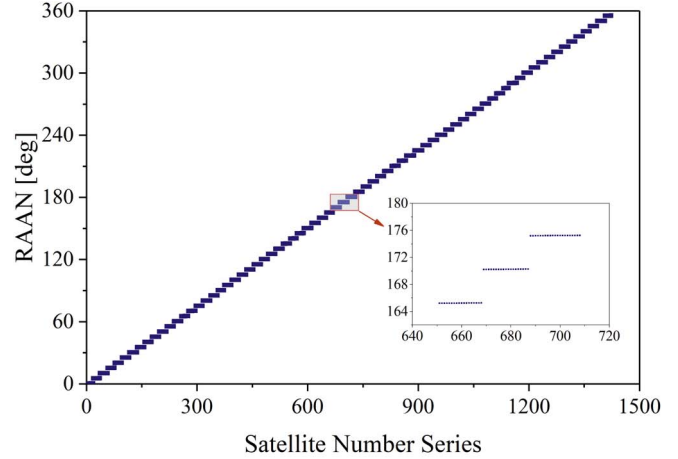
**Figure 4.** Distribution of the orbit semimajor axes and inclinations of 2566 Starlink satellites according to the TLE catalog (accessed on 2022 May 23).

550 km, and the whole raising process lasted more than 30 days. Specifically, after the launch, the satellites would stay at the initial orbit altitude of 350 km for several days, and this is called the adjusting period. After this period, the satellites start to climb sequentially, and this process, called the climbing period, would last for about 30 days. During the climbing period, the orbit altitudes of these satellites increase almost linearly, about 5.96 km/day, indicating that the thrust over a short time is almost the same for these satellites. The whole climbing process can be further examined by the variations of phase angles, as shown in Figure 6(b). At the beginning of the climbing period, the satellites are close to each other and then disperse gradually with time, as the phase angle of an individual satellite increases almost linearly. Eventually, these satellites climb to the destined orbit altitude of 550 km and are distributed evenly on the operational orbit, called the operational period. During the operational period, these satellites maintain their orbit altitude through orbit maneuvers to overcome the atmospheric drag effect.

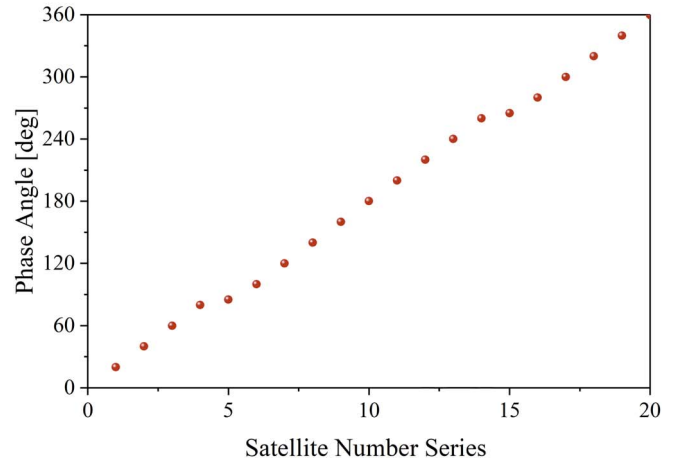
It is noted the Starlink satellites launched in different batches may have different climbing trends, but the satellites in the same orbital plane from the same launch share almost the same orbit variation characteristics.

#### 4.2. Object Matching

The tracklet-to-object matching of the climbing Starlink satellites starts with the rough matching, also called the initial matching, during which the NORAD TLEs are used to find the tracklets possibly belonging to cataloged objects. However, the accuracy of TLE-predicted positions drops quickly with time for the maneuvering satellites, resulting in the theoretical observations computed by the TLE-predicted positions containing large errors. Such errors could cause the mismatching or missed matching of tracklets. It is necessary to demonstrate the TLE validity time of the Starlink satellites by assessing the



(a) RAAN of orbital planes



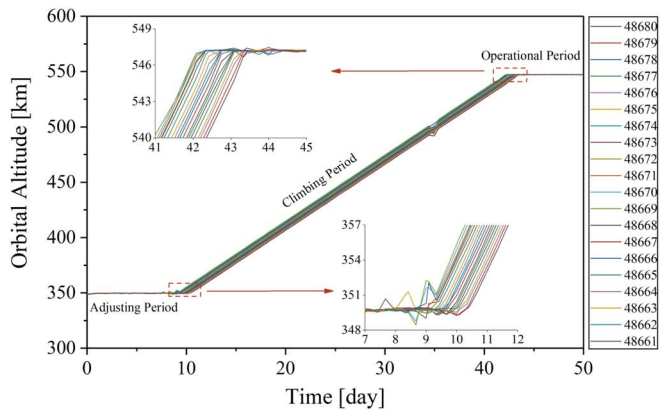
(b) Phase angles of satellites in an orbit

**Figure 5.** (a) Distribution of RAANs of the orbital planes of Starlink Satellites, and (b) phase angles of the satellites on the orbit of RAAN 20°2, orbital altitude 550 km, and inclination 53°0.

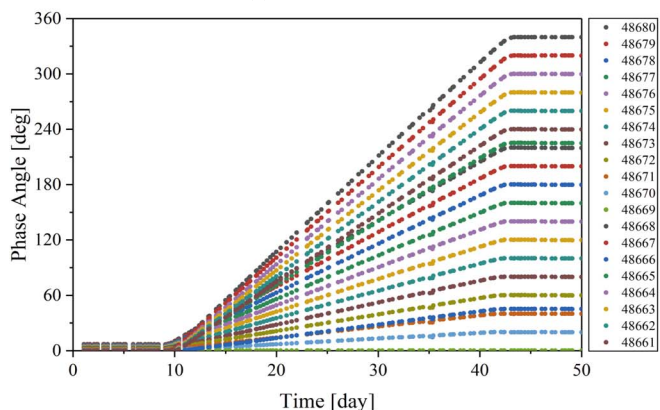
accuracy of TLE-predicted positions. Figures 7 and 8 present the TLE position prediction errors within 3 days of the TLE reference time for two Starlink satellites during the orbit climbing period and on the operational orbit, respectively, with the SpaceX ephemeris as reference.

In Figures 7 and 8, two important conclusions can be obtained. First, the along-track position prediction error  $e_S$  dominates the cross-track and radial position prediction errors,  $e_W$  and  $e_R$ ; second,  $e_S$  grows quickly with the prediction time, especially for the climbing Starlink satellites, with its maximum value reaching 10 km over 1 day and 150 km over 3 days. Such error growth trend demonstrates that the TLE-derived radar observations should be used very carefully in object matching. To guarantee the correct tracklet-to-object matching in the initial matching, the matching should be performed only to the tracklets within 1 day of the TLE





(a) Orbital altitude



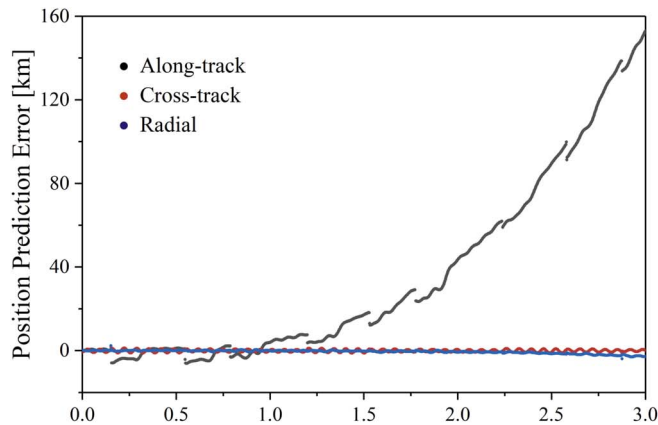
(b) Phase angle

**Figure 6.** Orbit variations of 20 deployed Starlink satellites during the climbing period. (a) Orbital altitude variations, and (b) phase angle variations

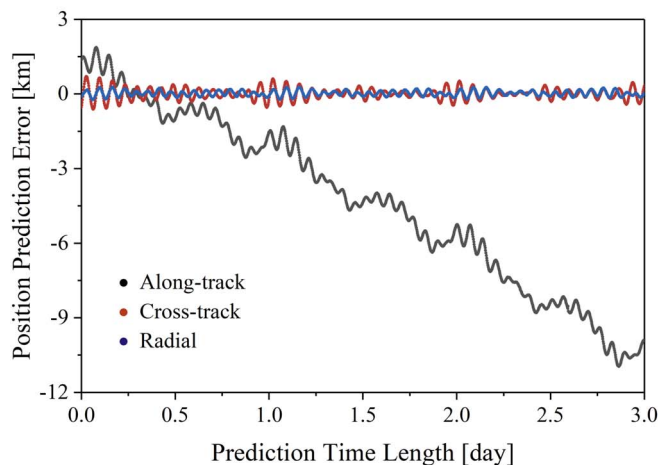
reference time. On the other hand, for the operational Starlink satellites,  $e_S$  over 1 day is at several kilometers, while it could reach dozens of kilometers over 3 days. Therefore, the same initial matching strategy should be applied for the operational satellites.

The TLE validity time is more clearly demonstrated using the rate of correct matching. There are 1931 tracklets collected within a 3 day time span for the 20 Starlink satellites in Figure 6, of which 1001 tracklets are for the climbing satellites and 930 tracklets are for the operational satellites. The last TLEs before the tracking are used to perform the initial matching. Considering the orbit features of Starlink satellites, the matching threshold is empirically fixed to  $1^\circ 0$  (equivalent to 18 km in the along-track direction at a distance of 1000 km between the station and the space object) for the angles and 10 km for the ranges. The correct matching rates during the climbing period and operational period are presented in Figure 9. The initial epoch is the TLE reference epoch.

Before assessing the tracklet-to-object matching performance with TLEs, the precise ephemerides of Starlink satellites



(a) during orbit climbing period



(b) on the operational orbit

**Figure 7.** TLE position errors of the Starlink satellite (NORAD ID: 48 675).

are used to determine the tracklets object attribution. In Figure 9, for the satellites in the operational orbit, the correct matching rate is about 85% in 1 day and then decreases slowly with time. When the TLE prediction time length extends to 2.5 days, the correct matching rate is less than 80%. In contrast, the correct matching rate for the climbing Starlink satellite is much low, at about 65% on the first day and 60% on the second day, but quickly drops to zero thereafter. Thus, the initial matching should be only performed for tracklets within 1 day of the TLE reference time.

Accurate orbits contribute to a high correct matching rate, and the orbit more accurate than the TLE orbit could be obtained by using the correctly matched tracklets in the initial matching. With the matched tracklets, the TLE orbit can be improved through the TLE-OD process, and then the improved TLE is used to find more tracklets. The orbit accuracy can be further improved with more correctly matched tracklets through the BLS OD which is based on

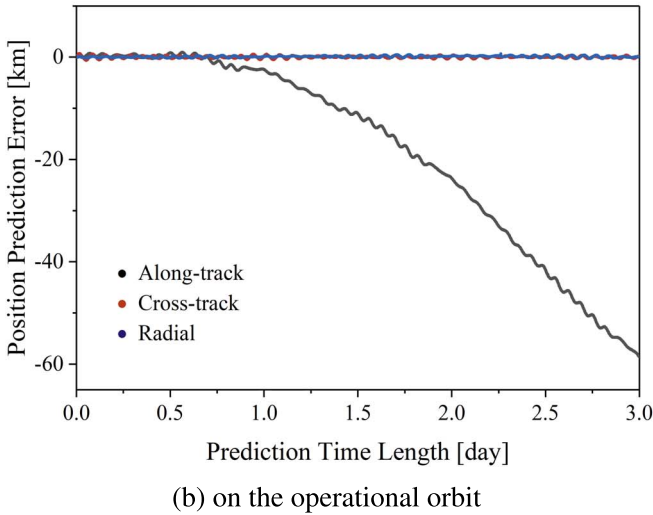
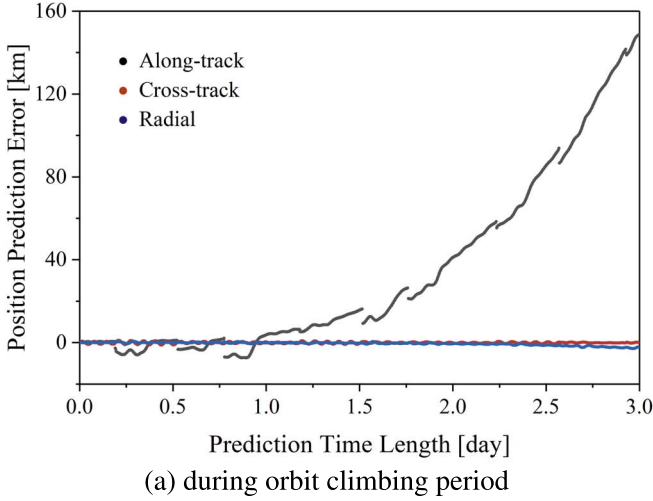


**Figure 8.** TLE position errors of the Starlink satellite (NORAD ID: 48 680).

more sophisticated dynamic models. Such a process can be referred to Figure 2. Figure 10 presents the position prediction accuracy of the NORAD TLE and its modification in each OD process (details for accurate OD with sparse tracklets will be given in Section 4.3).

It can be seen that, with more matched tracklets used in the OD, the prediction accuracy over 5 days improves significantly, from nearly 900 km at the beginning to about 450 km (in Figure 10(b)), to 38 km (in Figure 10(c)), and to only 7.1 km (in Figure 10(d)). Such great accuracy improvement demonstrates the effectiveness of the proposed OD methods. With more accurate OPs, the rate of correct tracklet-to-object matching is steadily at 100% over 5 days, as shown in Figure 11.

As Figure 11 reveals, the correct matching rate increases when a more accurate orbit is used. After the 1st OD improvement, the rate is 100% and 99.3% on the first and

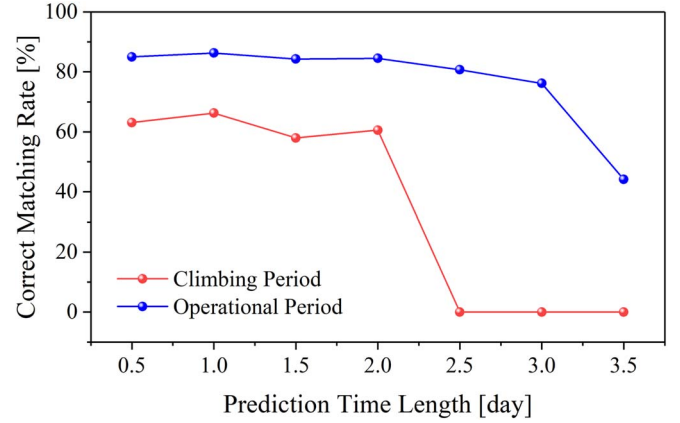


**Figure 9.** Correct matching rate with TLEs.

second day, respectively, but decreases to 49.8% on the fifth day. Surprisingly, after the 2nd OD improvement, the rate over 5 days is 100%, indicating that all the tracklets are correctly correlated to the right satellites. It can be seen that the use of the low-precision orbit causes poor tracking data utilization. Thus, in the practical data process, it is very important to perform the recursive tracklet-to-object matching for better data utilization.

#### 4.3. OD and OP with Sparse Tracklets

Through the tracking data analysis, it is found that the tracklets of almost every Starlink satellite are sparsely distributed if only a single station is operated. In fact, there are usually less than three tracklets for a satellite every day. Under the sparse data condition, the tracklet-to-object matching is even more crucial such that all the tracklets are found and used to help estimate the thrust effect in the BLS OD.

Here, a climbing Starlink satellite (NOARD ID: 48 675) is chosen to demonstrate the effectiveness of the proposed method of estimating thrust accelerations in the BLS OD. Through the tracklet-to-object matching, six tracklets are found belonging to the satellite over a 3-day span. A 3-day OD fit span is set starting from the beginning epoch of the first tracklet. During the OD span, the satellite orbit altitude rises from about 488.9 km to 506.8 km, according to the SpaceX ephemeris, while the orbit remains circular and at the same inclination, as shown in Table 1. In this case, the cross-track thrust model parameter is zero, that is,  $\Gamma_W = 0.0 \text{ m s}^{-2}$ . Only the along-track and radial thrust model parameters,  $\Gamma_S$  and  $\Gamma_R$ , are considered in the OD.

The last NORAD TLE before the OD fit span is used in the initial matching, and the tracklets on the first day are correctly matched. Use of the matched tracklets results in an improved TLE, with the TLE  $B^*$  being estimated to be  $-0.044459$ , different from the original  $-0.039759$ . Applying the

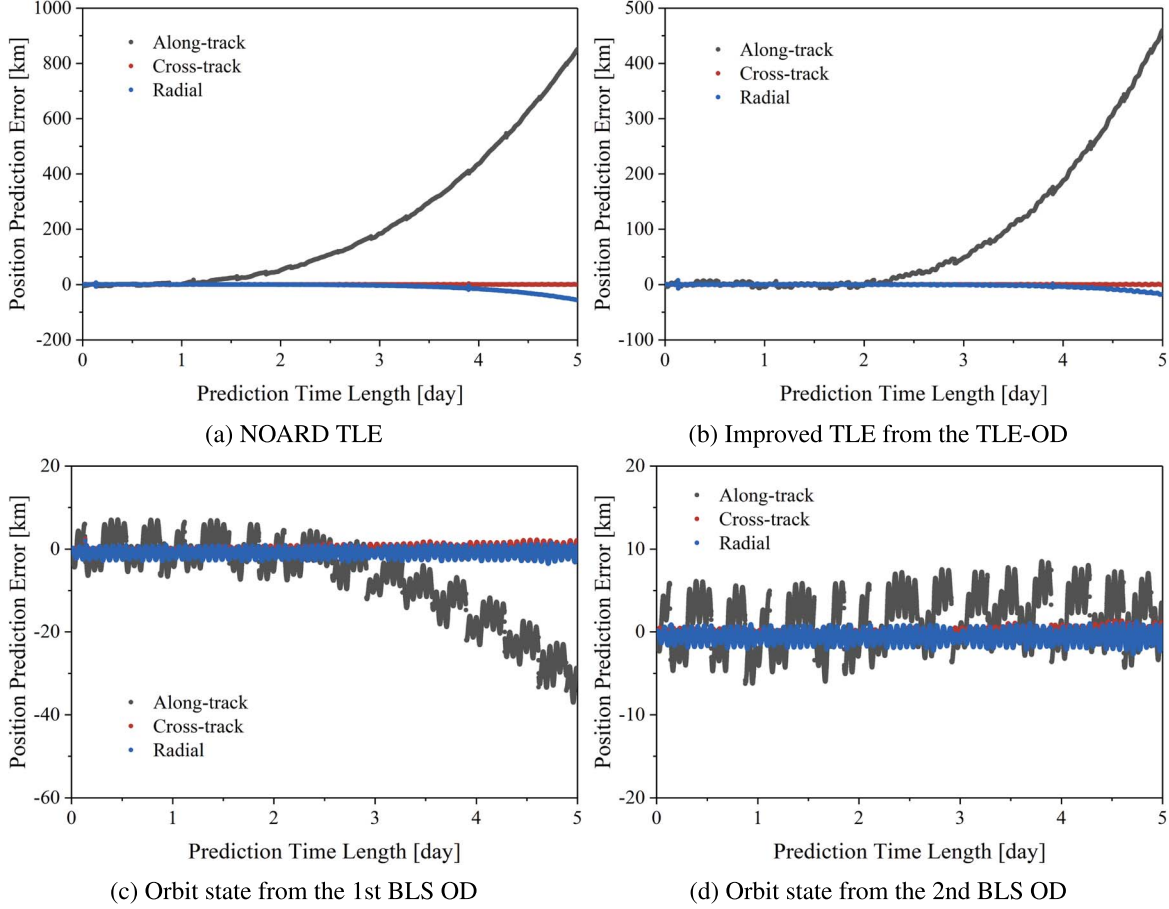


**Figure 10.** Errors of predicted positions using NORAD TLE and the improved ODs for a climbing Starlink satellite (NORAD ID: 48 675).

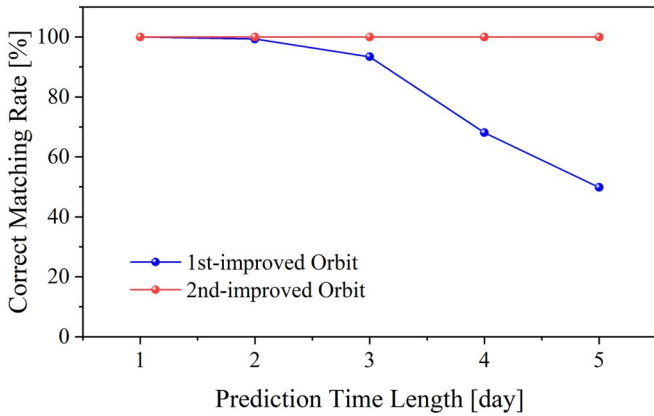


**Figure 11.** Correct matching rates for the climbing satellites with more accurate orbit predictions.

initialization method of thrust acceleration in Section 3.3, the initial value of  $\Gamma_S$  is determined as  $\Gamma_S^0 = -9.3 \times 10^{-4} \cdot B^* = 4.135 \times 10^{-5} \text{ m s}^{-2}$ .

With the tracklet in the last 0.5 days used as a reference,  $\max e_S$  values with respect to three values  $0.95 \times \Gamma_S^0$ ,  $\Gamma_S^0$ , and

$1.05 \times \Gamma_S^0$  can be obtained in the same way as that described in Section 3.3, and the linear fitting of the  $(\Gamma_S^0, \max e_S)$  series is shown in Figure 12. Therefore, a reasonably accurate initial value of  $\Gamma_S$  is obtained, and denoted as  $\bar{\Gamma}_S^0 = 3.939 \times 10^{-5} \text{ m s}^{-2}$ . It is noted that such initialization of  $\Gamma_S$  is crucial for the convergence of the OD process, when only sparse tracklets are available.

The initial orbit state for the accurate BLS OD is from the improved TLE, which helps accelerate the convergence of the OD process. Because the along-track thrust and the drag are hedged against each other, simultaneous estimation of  $\Gamma_S$  and  $C_d$  should be avoided. The whole BLS OD process is carried out in a few steps. In the first OD run,  $\Gamma_S$  is estimated, and  $C_d$  is fixed to 2.2. Two main reasons are behind such an orbit control approach: (1) the along-track thrust and drag are almost opposite to each other; and (2) in the low altitude region, the drag varies periodically because the satellite orbits pass through the Earth's shadow, while the along-track thrust is almost a constant over a few days.

The approach to estimating  $\Gamma_S$  in the BLS OD is similar to that in its initialization process. For this experiment case, only the sixth tracklet is in the last 0.5 days, which is used to compute the

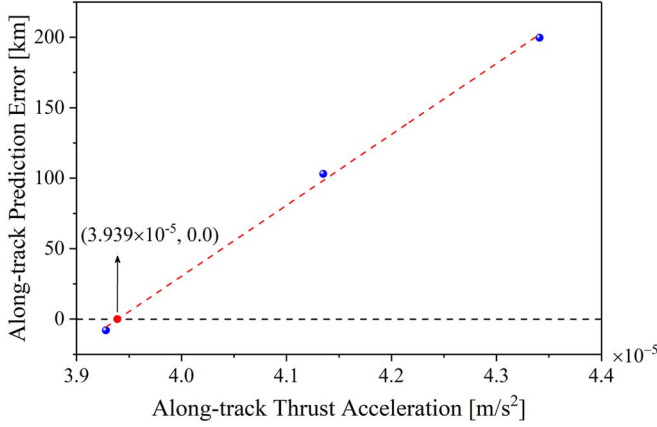


Figure 12. Accurate initialization of  $\Gamma_S$  for Starlink-48675.

along-track prediction error  $e_S$ . In this case, the prediction time length is the time span between the last epoch of the fifth tracklet and the last epoch of the sixth tracklet. Fixing  $\Gamma_S$  to  $0.95 \times \bar{\Gamma}_S^0$ ,  $\bar{\Gamma}_S^0$ , and  $1.05 \times \bar{\Gamma}_S^0$  in the BLS OD with only  $x_0$  and  $\Gamma_R$  as free parameters, respectively, the corresponding  $e_S$  values with respect to the sixth tracklet are obtained, as presented in Figure 13. It is noted that the time span between the fifth tracklet and the last tracklet is 0.65 days.

It is seen from Figure 13, although  $e_S$  varies with a given  $\Gamma_S$ , they are mostly at the same level over a short tracklet duration of about 87 s. Through linearly fitting ( $\Gamma_S, \max e_S$ ) series in Figure 13, an optimal estimate of  $\Gamma_S$  is obtained, and denoted as  $\hat{\Gamma}_S = 3.835 \times 10^{-5} \text{ m s}^{-2}$ . This value agrees very well with  $3.823 \times 10^{-5} \text{ m s}^{-2}$ , determined using the SpaceX ephemeris, with their relative error at about 0.3%. Experiments have shown that, such estimated  $\hat{\Gamma}_S$  is much more accurate than the one estimated from the OD with all tracklets.

After the estimation of  $\Gamma_S$ , the radial thrust acceleration  $\Gamma_R$  is estimated with all the tracklets during which  $\Gamma_S$  is fixed to  $\hat{\Gamma}_S$  and  $C_d$  to 2.2. The optimal estimation of  $\Gamma_R$  is  $3.510 \times 10^{-3} \text{ m s}^{-2}$ , that is,  $\hat{\Gamma}_R = 3.510 \times 10^{-3} \text{ m s}^{-2}$ .

Finally, given the thrust accelerations, ( $\hat{\Gamma}_S, \hat{\Gamma}_R$ ), an OD process with all the tracklets is performed again, in which  $C_d$  is estimated to absorb the unmodeled drag effect. After this OD, the orbit is predicted forward for only 2 days, since it is usually unknown whether the Starlink satellite continues to climb in the following days, and more importantly, the OP accuracy beyond 2 days degrades quickly. With the SpaceX ephemeris as the reference orbit, the position errors of OD and OP are computed, as presented in Figure 14.

As revealed in Figure 14, through precise modeling of the thrust, a much more accurate OP can be achieved for the climbing Starlink satellite, compared to the TLE-based OP shown in Figure 7(a) and Figure 8(a). Over the 2-day OP span,  $e_S$  dominates  $e_R$  and  $e_W$ , and is within  $[-8 \text{ km}, 8 \text{ km}]$ , while  $e_R$  and  $e_W$  are within  $[-3 \text{ km}, 2 \text{ km}]$ . However, the along-track

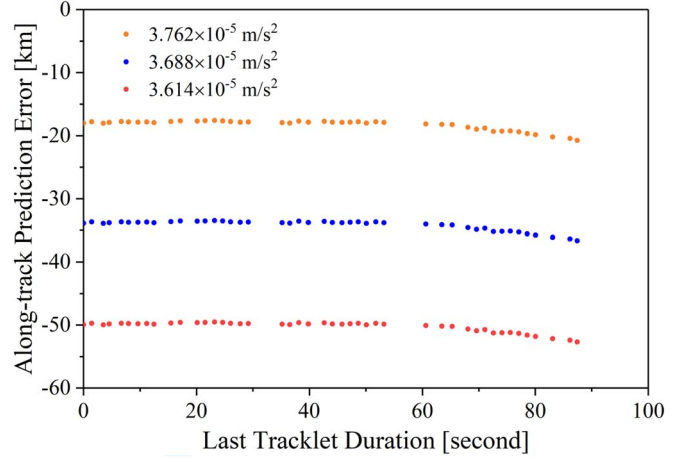


Figure 13. Varying  $\Gamma_S$  and corresponding  $e_S$  with respect to the last tracklet.

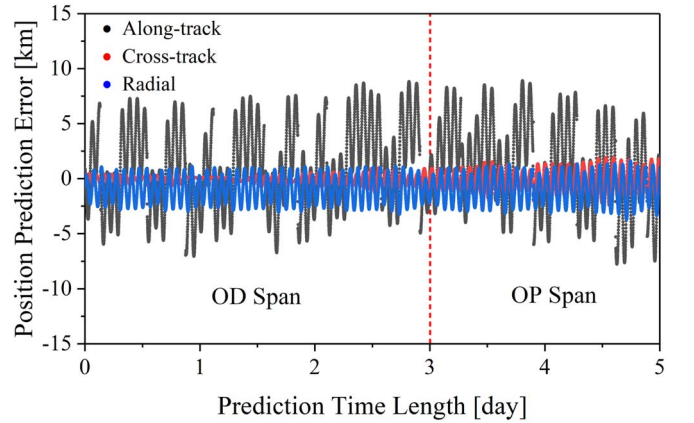


Figure 14. Position errors within the OD and OP spans.

errors in Figure 14 can be divided into 3–4 groups each day, with a clear jitter in error magnitude from one group to the next group. The jitter is caused by the discontinuity in the precise ephemeris. The jitters are also observed in Figures 10(c) and (d).

Similar OP accuracy is also achieved for 30 other climbing Starlink satellites, as shown in Figure 15. For each satellite, only sparse tracklets are available. Figure 15 presents the maximum values and rms values of the three-dimensional (3D) position prediction errors over 2 days of 30 maneuvering satellites.

The achieved 2-day OP accuracy for the climbing satellites is very satisfactory, with the maximum position prediction errors all less than 10 km. The rms values of 2-day 3D position prediction errors are all less than 6 km, mostly at the level of about 4 km. Compared to Figures 7(a) and 8(a) which show the 2-day errors of TLE-predicted along-track positions at the level of about 40 km, the OP errors are significantly reduced by the use of the developed algorithms, even with only 2–3 radar tracklets available each day. The fundamental reason is the appropriately estimated continuous thrust acceleration in the



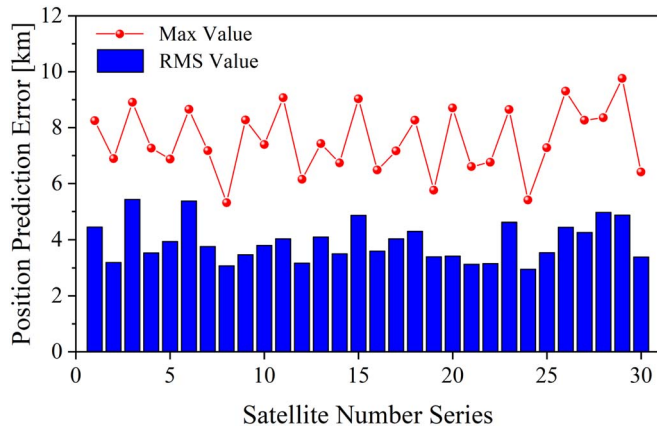


**Figure 15.** Position prediction errors over 2 days for 30 climbing Starlink satellites.

along-track direction. In fact, 2-day OP errors could reach tens of kilometers using the precise ephemeris and numerical integration method if the thrust is not considered or appropriately accounted for, as shown in Figure 3(a). The results in Figure 15 are the fair validation of the developed algorithms.

Such an OP performance is sufficiently accurate for quite a few SSA applications, such as box-based collision warnings, tracklet matching, and precision tracking schedules.

## 5. Conclusions

The growing population of Starlink satellites has made the LEO region much more crowded and poses serious threats to space assets. It requires accurate OP information of the Starlink satellites for high-precision SSA tasks. Although surveillance of Starlink satellites can yield a huge number of tracklets, how to correlate the tracklets with the right objects in the presence of maneuvers is still a challenge. Without correct tracklet-to-object matching, the accurate OD is almost impossible, especially for the maneuvering Starlink satellites.

This paper has developed a complete tracking data processing framework for climbing Starlink satellites. There are two critical parts in the framework, i.e., the tracklet-to-object matching, and estimation of the along-track thrust. To the problem of tracklet-to-object matching, a progressive matching approach is proposed which is based on the recursive OD and OP. In the initial matching using TLE, only the tracklets within 1 day of the TLE reference time are processed, and the matched tracklets are used to generate an improved TLE. The matching between the tracklets on the second day and the improved TLE orbit is then performed, and the orbit is further improved through the use of newly matched tracklets in the accurate BLS OD which considers full force models. It is shown the rate of correct tracklet-to-object matching is 100% for the climbing Starlink satellites. This paves the way for the accurate OD and OP.

To the problem of the along-track thrust estimation, a two-step approach is proposed. The key to this approach is to use the final tracklet as the control for the estimation of the along-track thrust. The first step, named the initialization, is to determine a reasonably accurate initial value of the along-track thrust from the  $B^*$  parameter in the improved TLE. Then, given the initial value and matched tracklets, an accurate value of the along-track thrust is determined through the BLS OD. Experiments have shown that the 2-day OP accuracy is at the level of a few km, even though the tracklets are usually sparse.

The developed tracking data processing framework has been shown very effective in the OD and OP process for the climbing Starlink satellites. The future study will focus on the orbit uncertainty propagation with the thrust model parameters, as well as the collision warning analysis for the mega-constellation of Starlink satellites.

## Acknowledgments

This research has been supported by the National Natural Science Foundation of China (Grant Nos. 12103035 and 41874035) and the Fundamental Research Funds for the Central Universities, China (Grant No. 2042021kf0001). The authors are grateful to anonymous reviewers whose constructive and valuable comments greatly helped us to improve the paper.

## ORCID iDs

Bin Li  <https://orcid.org/0000-0001-5548-0353>

## References

- Cai, H., Yang, Y., Gehly, S., Wu, S., & Zhang, K. 2018, *AcAau*, 151, 836  
 Dai, X., Lou, Y., Dai, Z., Hu, C., & Shi, C. 2019, *RemS*, 11, 1949  
 Goff, G. M., Black, J. T., & Beck, J. A. 2015, *AcAau*, 114, 152  
 Holzinger, M. J., Scheeres, D. J., & Alfriend, K. T. 2012, *JGCD*, 35, 1312  
 Huang, J., Hu, W.-D., Xin, Q., & Du, X.-Y. 2012, *RAA*, 12, 1402  
 Jiang, H., Liu, J., Cheng, H. W., & Zhang, Y. 2017, *RAA*, 17, 30  
 Kececy, T., & Jah, M. 2010, *AcAau*, 66, 798  
 Lee, S., Lee, J., & Hwang, I. 2016, *JGCD*, 39, 2034  
 Lei, X., Wang, K., Zhang, P., et al. 2018, *AdSpR*, 62, 542  
 Li, B., Huang, J., Feng, Y., Wang, F., & Sang, J. 2020, *ITAES*, 56, 4253  
 Li, B., Sang, J., & Ning, J. 2016, *AdAstroSci*, 158, 4003  
 Liu, L., Li, B., Chen, J. Y., et al. 2021, *RAA*, 21, 301  
 Montenbruck, O., & Gill, E. 2000, *Satellite Orbits—Models, Methods and Applications* (1st edn.; Berlin: Springer)  
 Picone, J., Hedin, A., Drob, D. P., & Aikin, A. 2002, *JGRA*, 107, A12  
 Qiao, Jing, & Chen, Wu 2018, *Gps Solutions*, 22, 42  
 Sang, J., Li, B., Chen, J., Zhang, P., & Ning, J. 2017, *AdSpR*, 59, 698  
 Serra, R., Yanez, C., & Frueh, C. 2021, *AcAau*, 181, 271  
 Siminski, J., Fiedler, H., & Flohrer, T. 2017, in *AAS/AIAA Space Flight Mechanics*, ed. J. W. McMahon et al. (San Antonio, TX: AAS/AIAA Space Flight Mechanics)  
 Standish, E. 1998, *F-98\_048*, 42  
 Tapley, B. D., Watkins, M., Ries, J., et al. 1996, *JGRB*, 101, 28029  
 Tu, R., Zhang, R., Zhang, P., et al. 2021, *Satellite Navigation*, 2, 1  
 Vallado, D. A. 2007, *Fundamentals of Astrodynamics and Applications* (3rd edn.; Hawthorne, CA: Microcosm Press)  
 Wang, X. H., Li, J. F., Du, X. P., & Zhang, X. 2016, *RAA*, 16, 139  
 Zhai, G., Bi, X., Zhao, H., & Liang, B. 2018, *Aerosp. Sci. Technol.*, 79, 352  
 Zhai, G. H. Z., Wen, Q., & Liang, B. 2019, *AcAau*, 162, 98